Available online at www.sciencedirect.com
SCIENCE DIRECT®
Journal of Solid State Chemistry 174 (2003) 104–110
JOURNAL OF SOLID STATE CHEMISTRY
http://elsevier.com/locate/jssc

Solid-phase photocatalytic degradation of polystyrene plastic with TiO_2 as photocatalyst

Jing Shang,[a] Ming Chai,[a] and Yongfa Zhu[a,b,*]

[a] *Department of Chemistry, Tsinghua University, Beijing 100084, China*
[b] *State Key Laboratory of C1 Chemical Technology, Tsinghua University, Beijing 100084, China*

Received 13 November 2002; received in revised form 9 March 2003; accepted 15 March 2003

Abstract

Solid-phase photocatalytic degradation of polystyrene (PS) plastic with TiO_2 as photocatalyst was investigated in the ambient air under ultraviolet light irradiation. Higher weight loss rate, lower average molecular weight, increased carbonyl peak intensity, less volatile organics and more CO_2 emitted with irradiation in PS-TiO_2 composite sample compared to pure PS sample were observed. These facts indicated the higher photodegradation rate of PS-TiO_2 sample than that of PS sample, and emphasized the potential of the composite sample in bring about complete photodegradation of polystyrene plastic. It is implied that the degradation initially occurred over TiO_2 particles, followed by the diffusion reaction with the aid of reactive oxygen species generated on TiO_2 particle surface.

Keywords: Polystyrene; Plastic; Photocatalytic degradation; TiO_2

1. Introduction

Plastic waste such as polystyrene (PS) disposal has been recognized as a worldwide environmental problem. Though various kinds of techniques have been proposed for the conversion of waste PS plastics, it is generally accepted that material recovery is not a long-term solution to the present problem [1]. Furthermore, even the manufacture of biodegradable and photodegradable (by the aid of addition of organic photosensitizer) plastics cannot solve the problem because these plastics have the limitation of long-term degradation and cause a different kind of environmental problem by the stabilizers introduced in their preparation [2]. Consequently, new technologies are being investigated for the degradation of plastic wastes. Thermal or catalytical degradation of waste PS plastics into fuel oils was investigated in recent years [1–4]. However, this technique requires not only high temperature and cost, but also appropriate catalysts to guarantee narrow distribution of hydrocarbons [4].

Heterogeneous photocatalytic oxidation reaction can occur at moderate conditions (room temperature, one atmosphere pressure and with molecular oxygen as the only oxidant) [5]. Due to the following characteristics: inexpensive, good photostability, non-toxicity, and high-reactivity, TiO_2 has proved itself to be the best photocatalyst. Photocatalysis technique has been widely used in the remediation of air and waste-water pollutants. However, waste plastics were usually exposed to the sunlight in an open air, so the degradation of plastics should be studied in solid-phase under the ambient air condition. Composition of plastics with TiO_2 presents a new way to decompose solid plastics in an open air. There are few reports on the solid-phase photocatalytic oxidation process [6]. Only one reference is given. In this paper, solid-phase photocatalytic oxidation of PS with TiO_2 as photocatalyst under ultraviolet (UV) light irradiation was firstly investigated. The process of photocatalytic oxidation of PS-TiO_2 composite sample was compared with that of photooxidation of PS sample. The solid-phase photocatalytic oxidation mechanism of PS-TiO_2 composite sample was discussed.

*Corresponding author. Fax: +86-10-62787601.
E-mail address: zhuyf@chem.tsinghua.edu.cn (Y. Zhu).

0022-4596/03/$ - see front matter © 2003 Elsevier Science (USA). All rights reserved.
doi:10.1016/S0022-4596(03)00183-X

2. Experimental

2.1. Materials

PS, coming from one-off plastic appliance commercially available, was chosen in the experiment. The weight average molecular weight (M_w) was determined by gel permeation chromatography (GPC) (HP 1100) to be around 84100. The TiO_2 photocatalyst was prepared by sol–gel method with $TiCl_4$ as precursor. $TiCl_4$ of 2.0 mL was slowly added dropwise into 15 mL ethanol solution at room temperature. Then a light yellow solution was obtained and gelatinized for 3 days to form a sol. After drying, the sample was calcinated at 673 K for 3 h. X-ray analysis (Bruker D8 Advance powder diffractometer with Cu$K\alpha$ source) of the TiO_2 powder revealed the formation of anatase only and the mean crystallite size was estimated to be 13.2 nm using the Scherrer equation [7].

2.2. Preparation and characterization of PS-TiO_2 composite film

PS-TiO_2 composite film sample was cast as follows. Dissolving 0.5 g of one-off plastic appliance in 10 mL of tetrahydrofuran (THF) under vigorous stirring for 30 min. Then 0.01 g of the TiO_2 powder was suspended uniformly in the above 10 mL solution to give 2.0 wt% of TiO_2 content with respect to the total mass of PS. An aliquot of 10 mL PS-TiO_2 solution was spread on a polytetrafluoroethylene plate (15 cm × 15 cm) and dried for 48 h at room temperature. The thickness of the resulting PS-TiO_2 composite film sample was measured to be 35 μm by SEM. The pure PS sample and the PS-TiO_2 composite sample before and after irradiated at different time were all characterized by means of GPC, FT-IR, XPS and SEM techniques. The average molecular weight of the PS-TiO_2 and PS-(TiO_2/CuPc) composite samples were determined by GPC (HP 1100) equipped with a PL mixed C (×2) column and a refractive index detector. PS standards were used for the M_w calibration. For GPC analysis, all the samples were dissolved in THF, then filtered through a 0.2 μm PTFE syringe filter in order to remove TiO_2 particles. FT-IR patterns were acquired from a Perkin-Elmer System 2000 infrared spectrameter. The XPS spectra were measured in a PHI 5300 ESCA system. During XPS analysis, a Al $K\alpha$ X-ray beam was used, and the power was set at 250 W. A hemispherical analyzer with a position sensitive detector at a pass energy of 35.75 eV was also used. The base vacuum of chamber was maintained at 3×10^{-9} Torr during XPS analysis. The morphologies of the samples were taken by using SEM (KYKY, 2000).

2.3. The photooxidation and photocatalytic oxidation of PS and PS-TiO_2 samples

The photooxidaion reaction occurred under ambient air in a lamp-housing box (40 cm × 30 cm × 20 cm) where the temperature during irradiation was maintained around 298 K. PS and PS-TiO_2 samples were irradiated under four 8 W ultraviolet lamps. The primary wavelength distribution of the lamps is at 253.7 nm and the light intensity is measured to be 2.5 mW/cm^2 at 5 cm away from the lamps. A typical size of the film sample was about 100 cm^2. The volatile organics generated during the photooxidation of PS and PS-TiO_2 samples were detected by a gas chromatograph (GC) equipped with a flame ionization detector (FID) and GDX-403 steel column. In experiment, one stage temperature programming was set: the initial oven temperature was 313 K, then raised at a rate of 40 K/min to final temperature 373 K. The initial and final time was 1 and 5 min, respectively. The volatile organics were identified individually by standard samples which were provided by Beijing AP BAIF Gases Industry Limited. The concentration of CO_2 was measured by GC equipped with a thermal conductivity detector (TCD) using GDX-403 steel column at 343 K.

3. Results and discussion

3.1. Weight loss and the decrease of molecular weight (M_w)

Fig. 1(A) shows the photoinduced weight loss of pure PS sample and PS-TiO_2 composite sample in air under UV irradiation. The weight loss rate was much higher for the PS-TiO_2 than for pure PS sample. The weight of the PS-TiO_2 sample steadily decreased with irradiation and led to the total 22.5% reduction in 150 h, while the PS sample showed only 12.0% weight loss at the same experimental condition.

Fig. 1(B) displays the variations of molecular weight (M_w) of the pure PS sample and PS-TiO_2 composite sample with irradiation time. It can be seen from Fig. 1(B) that before irradiation, the M_w for two samples are almost the same. After UV lamps were turned on, the average M_w of the two samples both decreased. But the decreasing extent of M_w for composite film sample was larger than that for pure film sample. The reduced percents of average M_w for PS and PS-TiO_2 sample after 200 h irradiation was about 67% and 85%, respectively. Above results indicate that the bond scission in the backbone of the composite polymer is ascribed to both the direct photolytic and the photocatalytic reaction. It is observed from Fig. 1(B) that the M_w rapidly decrease during the initial stage of irradiation. This behavior may be due to main-chain scission. In polymer degradation

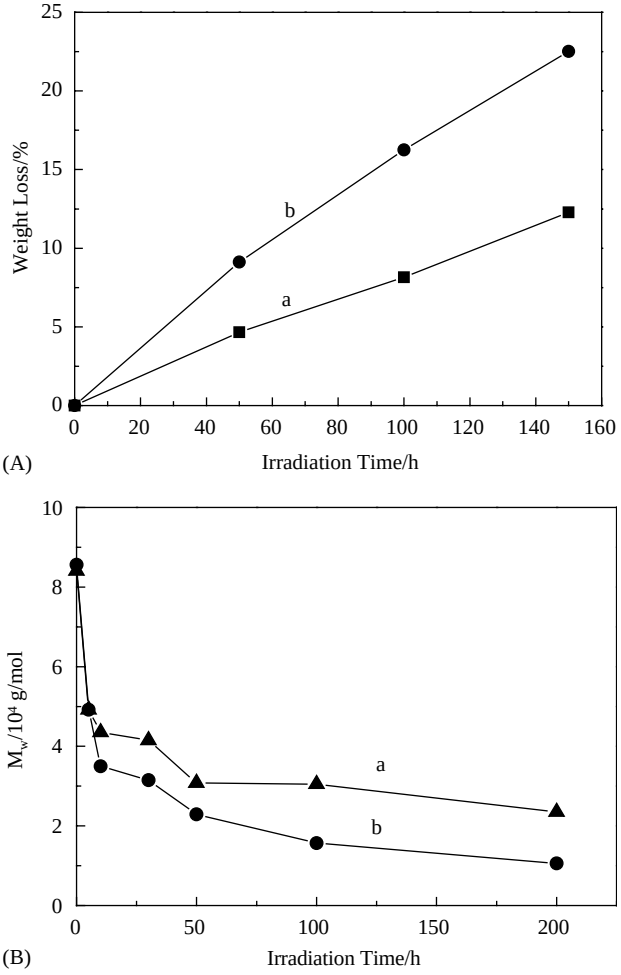

Fig. 1. (A) Weight loss of PS (a) and PS-TiO_2 (b) samples with irradiation time. (B) The variations of average molecular weight M_w of PS (a) and PS-TiO_2 (b) samples with irradiation time.

where chain scission occurs at random, one always can see a rapid initial molecular weight decrease, which slows down as the process continues.

3.2. Photodegradation species on the sample surface

The facts that the weight loss and M_w decrease imply that there must be degradation reaction occurred during irradiation. Fig. 2 compares the FT-IR spectra of both PS and PS-TiO_2 samples after irradiated for 30 h with that of original PS sample. It should be noted that there are nearly no differences in the IR spectra with its wavenumbers range from 2000 to 600 cm^{-1} for original PS and PS-TiO_2 composite samples, so the comparison is reasonable. This also indicates that interaction between PS and TiO_2 is physical, not chemical. The IR spectrum of pure PS sample presents the characteristic peaks of phenyl ring at 697, 756, 1028, 1450 and 1492 cm^{-1}. The irradiated PS and PS-TiO_2 samples show much lower intensity of phenyl ring characteristic

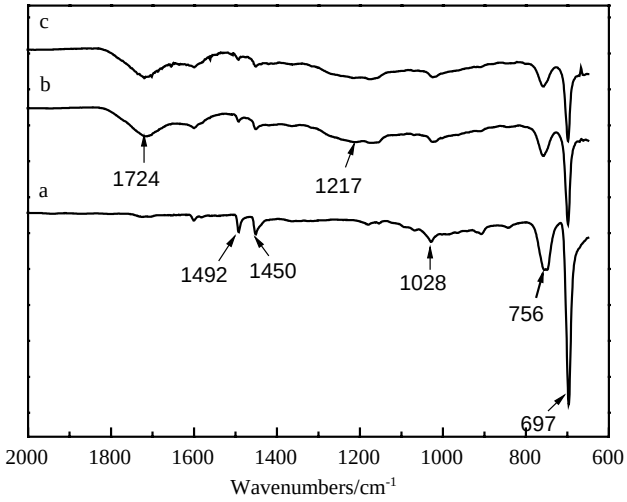

Fig. 2. The FT-IR spectra of PS sample before irradiation (a), PS sample irradiated for 30 h (b) and PS-TiO_2 sample irradiated for 30 h (c).

peaks compared with the original PS sample, especially the strong peaks at 697 and 756 cm^{-1}. Furthermore, the decreased extent for composite sample is higher than that for pure sample. The decrease of the characteristic peaks can be responsible for the phenyl ring opening reactions in PS [8,9]. There are two new peaks at the position of 1724 and 1217 cm^{-1} of the irradiated two samples, which can be assigned to C═O [10] and C–O [11] stretching vibrations, respectively.

Fig. 3(A) and (B) show XPS spectra of C 1s and O 1s of PS samples before and after irradiation, as well as those of the irradiated PS-TiO_2 composite sample. Based on the peak-fitting results of C 1s (Fig. 3(A)), there are two peaks for original PS sample at 284.8 eV (peak 1) and 288.2 eV (peak 2), respectively. Peak 1 can be assigned to –C–C– group, and peak 2 is attributed to the carboxyl group of plasticizers. The content of peak 2 increases from 16.33% (a in Fig. 3(A)) to 31.75% (b in Fig. 3(A)), indicating some other species containing carboxyl group formed after irradiation. The irradiated PS and PS-TiO_2 samples present a new peak at 286.5 eV (peak 3), which is an indication of the existence of –C–O group, implying the presence of alcohols and carboxylic acids [12]. The content of peak 3 for irradiated PS-TiO_2 sample (46.87%) is higher than that of irradiated PS sample (10.99%), implying the reaction rate of composite sample is much higher than that of pure PS sample The extended peak at 289.6 eV (peak 4) for irradiated composite sample can be estimated to be further oxidation products including –COO group, indicative of the presence of polycarbonate, carboxylic acids or carboxylates [12,13]. Based on Fig. 3(B), the initial PS sample surface showed the presence of oxygen at the binding energy of 532.3 eV (peak 1), which is assigned to typical oxygen groups such as carbonyl and OH [6]. For

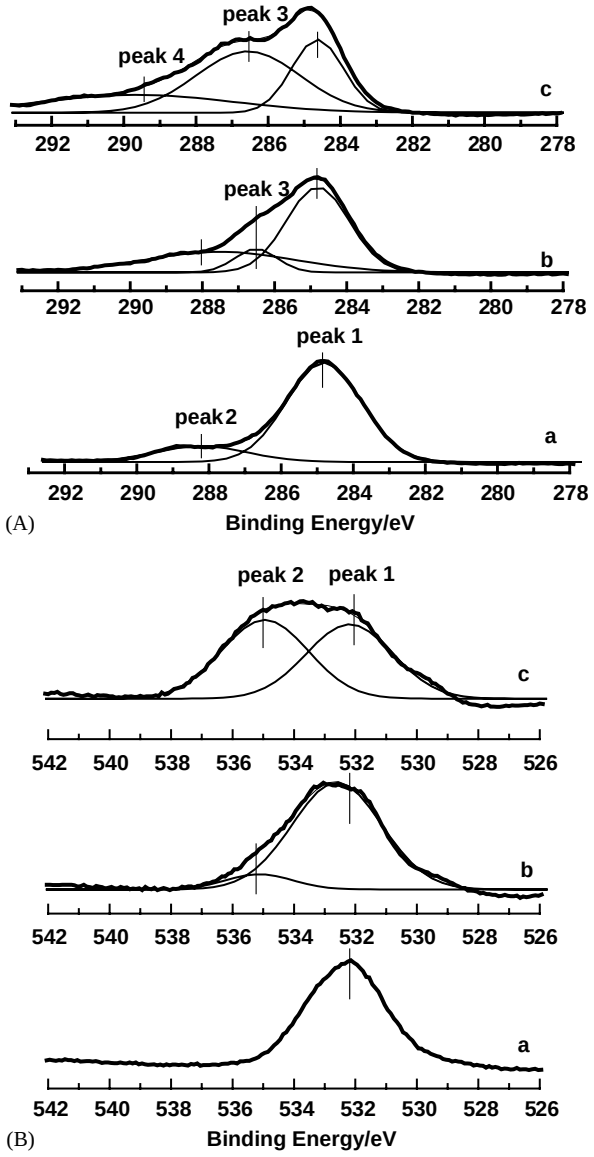

Fig. 3. High-resolution XPS spectra of C 1 s (A) and O 1 s (B) of PS sample before irradiation (a), PS sample irradiated for 130 h (b) and PS-TiO_2 sample irradiated for 130 h (c).

irradiated PS and PS-TiO_2 samples, a new peak at 535.1 eV (peak 2) was occurred, which can be attributed to carbonate –OCO_2– or carboxylic acids. The content of peak 2 increased from 9.63% to 51.61%, indicating these species were produced much faster on the surface of composite sample than on that of PS sample. XPS results are in agreement with that of IR, which both indicated the formation of the carbonyl and carboxyl groups on the surface of irradiated PS-TiO_2 samples.

3.3. Morphology of samples after photodegradation

The morphologies of irradiated polymer samples were carried out by using scanning electron microscopic (SEM) analysis. Fig. 4(A) and (B) show the morphologies of PS and PS-TiO_2 samples that were irradiated for 0, 5 and 40 h in air, respectively. After irradiated for 5 h, the hole density of pure PS sample is about 0.8 μm^{-2} and hole diameter being less than 1 μm; while for PS-TiO_2 sample, the hole number density is about 1.1 μm^{-2} and hole diameter is about 1–1.5 μm. The formation of the holes may come from the escape of volatile organics from PS matrix. After irradiated for 40 h, the pure PS sample appears bigger hole with its maximal diameter about 3.0 μm, while the hole density remains unchanged. For PS-TiO_2 composite sample, the individual cavity got highly inter-connected after irradiated for 40 h and coalesced to a size of about 3.1 μm. The SEM images revealed that photooxidation reactions were performed on the surface of irradiated PS sample. When TiO_2 was added, the degradation of PS matrix started from the PS-TiO_2 interface and led to the formation of cavities around TiO_2 particle aggregates. It is implied that the active oxygen species generated on TiO_2 surface desorb and diffuse through a finite distance to etch out the polymer matrix.

3.4. The formation of carbon dioxide and volatile organics during photodegradation of PS and PS-TiO_2 samples

GC equipped with TCD or FID was used to measure the amount of carbon dioxide and volatile organics produced during the photooxidation process, respectively. Fig. 5 shows variations of the concentration of carbon dioxide with irradiation time. For PS sample the concentration of CO_2 increased with irradiation time and then became stable after irradiated for 4 h. While for PS-TiO_2 sample, the concentration of CO_2 increased continuously. The formation of CO_2 in pure PS case was due to the photolysis of plasticizers, and saturation was reached after irradiated for 3.5 h. For PS-TiO_2 case, CO_2 come not only from the photolysis of plasticizers but also from the photocatalytic degradation of PS, so its amount ascended during the irradiation.

In Fig. 6(A), curve g is peaks of the volatile organics identified by GC. Peak 1 can be attributed to the air peak. Peaks 2–7 are the volatile organics generated during the photooxidation process. Curves a–f refer to GC peaks of ethene, ethane, butane, acetaldehyde, formaldehyde and ethanol standard samples, respectively. It can be seen that peaks 2–7 exhibit the same reserve time as that of a–f, respectively. The good consistency of the reverve time of volatile organics with that of standard gases can always be obtained no matter what the oven temperature is. Therefore, the generated volatile organics are ethene, ethane, butane, acetaldehyde, formaldehyde and ethanol. Fig. 6(B) compares the total area of these volatile organics for PS and PS-TiO_2 samples with irradiation time. It is interesting to note

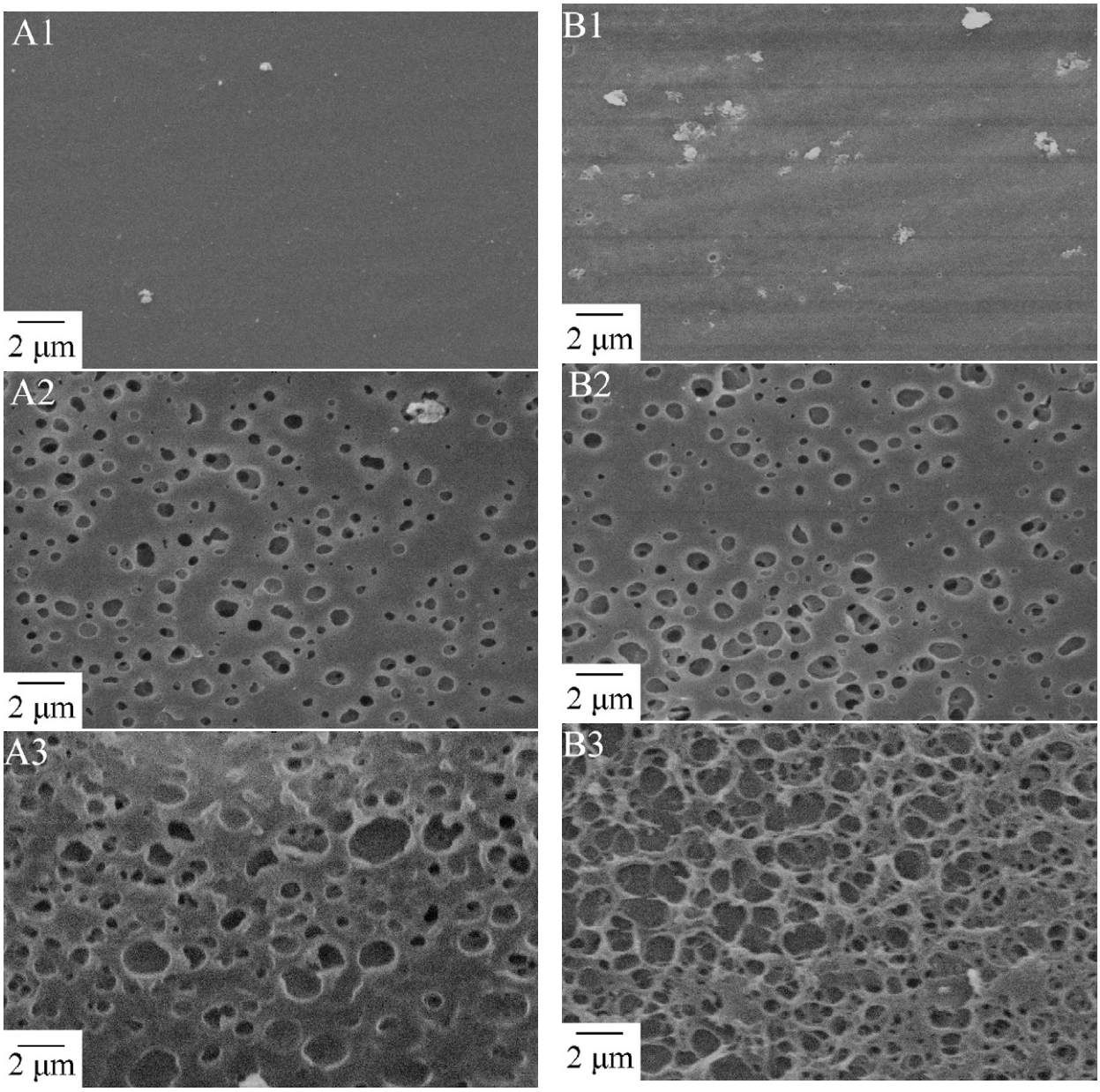

Fig. 4. SEM images of PS (A) and PS-TiO_2 (B) samples. (A1): PS sample before irradiation; (A2): PS sample irradiated for 5 h; (A3): PS sample irradiated for 40 h; (B1): PS-TiO_2 sample before irradiation; (B2): PS-TiO_2 sample irradiated for 5 h; (B3): PS-TiO_2 sample irradiated for 40 h.

that the amount of organics emitted by PS-TiO_2 sample is always less than that by PS sample in various irradiation time, though the reaction rate of composite sample is higher than the pure sample. For PS sample, photolysis products such as volatile organics are accumulated, due to its weak capacity of deep mineralization. While for PS-TiO_2 composite sample, the generated volatile organics such as aldehydes and ethanol can occur complete mineralizaion by photocatalytic oxidation reactions [14], with less volatile organics left and more CO_2 formed. This indicates that PS-TiO_2 composite sample has the potential to proceed complete photodegradation of PS plastic, rather than simple photolysis of PS sample.

3.5. *Solid-phase photocatalytic oxidation mechanism of PS-TiO_2 composite sample*

Based on above results, it can be known that both PS-TiO_2 and PS samples can proceed photolysis under ambient air. Previous works [8,9,15–18] indicated reaction of PS under ultraviolet irradiation occurred via direct absorption of photons by the PS macromolecule to create excited states, and then undergo

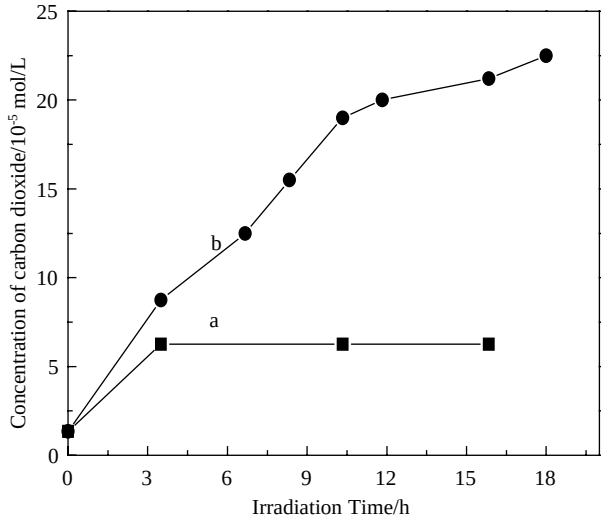

Fig. 5. The variations of concentration of CO_2 for PS (a) and PS-TiO_2 (b) samples with irradiation time.

chain scission, branching cross-linking and oxidation reactions. The composite sample showed better photodegradation reactivity than that of pure PS sample. For composite sample, there was not only the photolytic reaction of PS but also the photocatalytic reaction of PS on the surface of TiO_2. However, the initiation in the photocatalytic degradation of PS-TiO_2 composite sample is quite different from that of pure PS sample. The photocatalytic reaction mechanism of PS-TiO_2 can be written as followed. When a photon with energy of $h\upsilon$ matches or exceeds the band-gap energy of TiO_2 particles, the conduction-band electrons (e^-) and valence-band holes (h^+) generate on the surface of TiO_2 (Eq. (1)). In the absence of the electron and hole scavengers, most of them recombine with each other within a few nanoseconds. If the scavengers or surface defects are present to trap the electron or hole, e^-–h^+ recombination can be prevented and the subsequent reactions caused by the electrons and holes may be dramatically enhanced [19]. In this case, oxygen adsorbed on the surface of TiO_2 plays significant role in the reaction with electrons, with O_2^-, O and O^- being the products of electron transfer (Eqs. (2)–(4)) [20]. At the same time, photogenerated holes are trapped by hydroxyl ions or water adsorbed on the surface, producing hydroxyl radicals (Eqs. (5) and (6)), which play important roles in photocatalytic reactions [12].

$$TiO_2 \xrightarrow{h\upsilon} TiO_2(e^- + h^+), \quad (1)$$

$$O_{2ads} + e^- \rightarrow O_{2ads}^-, \quad (2)$$

$$O_{2ads} \rightarrow 2O_{ads}, \quad (3)$$

$$O_{ads} + e^- \rightarrow O_{ads}^-, \quad (4)$$

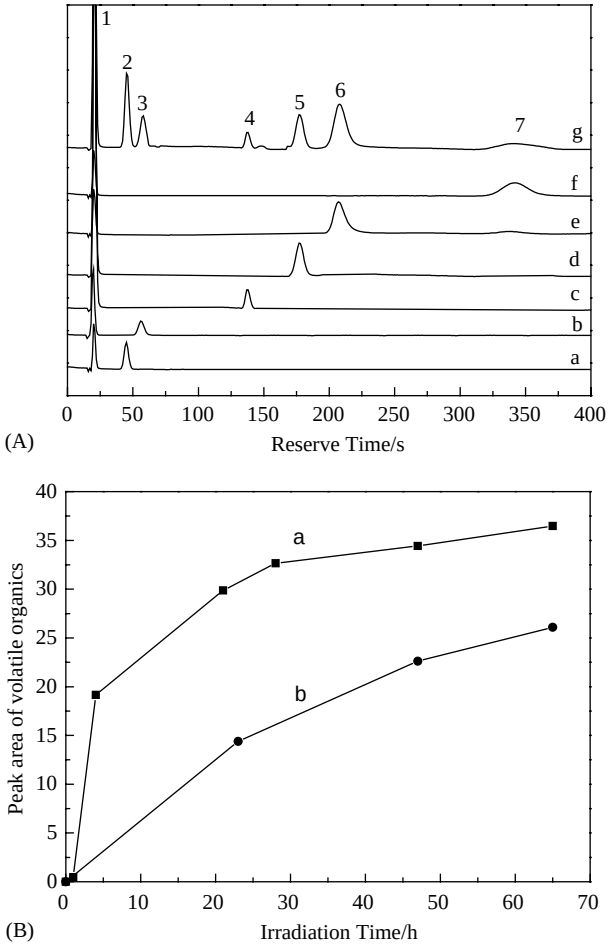

Fig. 6. (A) Curves a–f refer to GC peaks of ethene, ethane, butane, acetaldehyde, formaldehyde and ethanol standard samples, respectively; curve g is GC peaks of volatile organics. (B) The total area of the volatile organics for PS (a) and PS-TiO_2 (b) samples with irradiation time.

$$OH^- + h^+ \rightarrow {}^{\bullet}OH, \quad (5)$$

$$H_2O_{ads} + h^+ \rightarrow {}^{\bullet}OH + H^+, \quad (6)$$

$$-(CH_2CHPh)- + {}^{\bullet}OH \rightarrow -(CH_2\dot{C}Ph)- + H_2O, \quad (7)$$

$$-(CH_2CHPh)- + {}^{\bullet}OH \rightarrow -(\dot{C}HCHPh)- + H_2O, \quad (8)$$

$$-(CH_2\dot{C}Ph)- + O_2 \rightarrow -(CH_2C(O\dot{O})Ph)-, \quad (9)$$

$$-(\dot{C}HCHPh)- + O_2 \rightarrow -(CH(\dot{O}O)CHPh)-, \quad (10)$$

$$-(CH_2C(O\dot{O})Ph)- + -(CH_2CHPh)- \rightarrow -(CH_2C(OOH)Ph)- + -(CH_2\dot{C}Ph)-, \quad (11)$$

$$-(CH(\dot{O}O)CHPh)- + -(CH_2CHPh)- \rightarrow -(CH(OOH)CHPh)- + -(CH_2\dot{C}Ph)-, \quad (12)$$

$$-(CH_2C(OOH)Ph)- \rightarrow -(CH_2COPh)- + {}^{\bullet}OH, \quad (13)$$

$$-(CH(OOH)CHPh)- \rightarrow -(CHOCHPh)- + {}^{\bullet}OH, \quad (14)$$

$$-(CH_2COPh)-(\text{or}-(CHOCHPh)-) + O_2, \xrightarrow{TiO_2,h\upsilon} \text{intermediates such as PhCOOH, PhCHCOOH, aldehydes and ethanol}$$

$$\xrightarrow{TiO_2,h\upsilon} \text{chain scission with } CO_2 \text{ evolution} \quad (15)$$

Moreover, reactions among O_2^-, O and H_2O_{ads} give rise to the formation of $^{\bullet}OH$ and HO_{2ads}, which is another source of $^{\bullet}OH$ [14,21]. The reactive oxygen species described above initiate the degradation reaction by attacking neighboring polymer chains (Eqs. (7) and (8)). The degradation process spatially extends into the polymer matrix through the diffusion of the reactive oxygen species. Once the carbon-centered radicals are introduced in the polymer chain, their successive reactions lead to the chain cleavage with the oxygen incorporation and species containing carboxyl and carbonyl groups such as CH_2COPh, CHOCHPh, PhCOOH and PhCHCOOH produced (Eqs. (9)–(15)). Phenyl ring can also be detached from the polymer to form volatile organics such as aldehydes and ethanol. These intermediates can be further photocatalytically oxidized to CO_2 and H_2O by the aid of reactive oxygen species.

4. Conclusions

1. The photocatalytic degradation process of PS-TiO_2 composite sample was much faster than the simple photolysis of pure PS sample.
2. The solid-phase photocatalytic oxidation of PS sample was initiated by reactive oxygen species generated on TiO_2 surface. The further reactions involving these reactive oxygen species result in some by-products containing carbonyl and carboxyl groups and the final products CO_2.
3. The development of this new kind of composite polymer that proceed degradation under ambient sunlight irradiation with little formation of toxic by-products can lead to an eco-friendly disposal of polymer wastes. The polymer-TiO_2 composite has a potential viability to be used as a photodegradable product.

Acknowledgments

This work was supported by Chinese National Science Foundation (20071021), Excellent Young Teacher Program of MOE, People' Republic of China and Visiting Scholar Foundation of Key Lab in Beijing University.

References

[1] S.Y. Lee, J.H. Yoon, J.R. Kim, D.W. Park, Polym. Degrad. Stab. 74 (2001) 297.
[2] S.Y. Lee, J.H. Yoon, J.R. Kim, D.W. Park, J. Anal. Appl. Pyrol. 64 (2002) 71.
[3] T. Faravelli, M. Pinciroli, F. Pisano, G. Bozzano, M. Dente, E. Ranzi, J. Anal. Appl. Pyrol. 60 (2001) 103.
[4] D. Dong, S. Tasaka, N. Inagaki, Polym. Degrad. Stab. 72 (2001) 345.
[5] J. Peral, X. Domenech, D.F. Ollis, J. Chem. Technol. Biotechnol. 70 (1997) 117.
[6] S. Cho, W. Choi, J. Photochem. Photobiol. A 143 (2001) 221.
[7] H. Ogawa, A. Abe, J. Electrochem. Soc. 128 (1981) 685.
[8] H. Kaczmark, Eur. Polym. J. 31 (1995) 1037.
[9] H. Kaczmark, A. Kaminska, M. Swiatek, S. Sanyal, Eur. Polym. J. 36 (2000) 1167.
[10] F. Fally, I. Virlet, J. Riga, J.J. Verbist, J. Appl. Polym. Sci. 59 (1996) 1569.
[11] L.A. Phillips, G.B. Raupp, J. Mol. Catal. A 77 (1992) 297.
[12] Y.J. Zhu, N. Olson, T.P. Beebe, Environ. Sci. Technol. 35 (2001) 3113.
[13] M.M. Chehimi, M.L. Abel, J.F. Watts, R.P. Digby, J. Mater. Chem. 11 (2001) 533.
[14] V. Augugliaro, S. Voluccia, V. Loddo, L. Marchese, G. Martra, L. Palmisano, M. Schiavello, Appl. Catal. B 20 (1999) 15.
[15] A.G. Rincon, Polym. Bull. 38 (1997) 191.
[16] K.D. Crawford, K.D. Hughes, J. Phys. Chem. B 101 (1997) 864.
[17] H. Kaczmark, Eur. Polym. J. 31 (1995) 1175.
[18] S.I. Kuzina, A.I. Mikhailov, Eur. Polym. J. 34 (1998) 291.
[19] D.R. Park, J.L. Zhang, K. Ikeue, H. Yamashita, M. Anpo, J. Catal. 185 (1999) 114.
[20] J. Peral, D.F. Ollis, J. Catal. 136 (1992) 554.
[21] E. Pellizzetti, C. Minero, Electrochim. Acta 38 (1993) 47.